1966

A study of the effects of ultrasonics on self-diffusion of zinc

Brian F. Walker
Lehigh University

A STUDY OF
THE EFFECTS OF ULTRASONICS
ON SELF-DIFFUSION OF ZINC

by

Brian F. Walker

A Thesis

Presented to the Graduate Faculty

of Lehigh University

in Candidacy for the Degree of

Master of Science

Lehigh University

1966

CERTIFICATE OF APPROVAL

This thesis is accepted and approved in partial fulfillment of the requirements for the degree of Master of Science.

23 May 1966
Date

Advisor

Advisor

Head of the Department of
Metallurgical Engineering

ACKNOWLEDGMENTS

The author wishes to express his gratitude to Dr. John D. Wood and Dr. Walter C. Hahn for their guidance and constructive criticism throughout this investigation. Appreciation is extended to the many people of the Western Electric Company Engineering Research Center of Princeton who have counseled and aided me in so many ways. In particular, sincere thanks are offered to Mr. R. B. Palme, Mr. M. J. Brown, Mr. B. K. Reid, Mr. R. E. Thomas, and Mr. J. W. Rice for their assistance and advice throughout various stages of this investigation.

My gratitude is also expressed to my wife for her patience, understanding, and encouragement during this investigation.

TABLE OF CONTENTS

LIST OF FIGURES

ABSTRACT

Previous studies have indicated enhanced solid state diffusion with the application of ultrasonic energy. A direct measurement of this enhancement was attempted for the case of self-diffusion in zinc. Using radioactive tracer techniques, the diffusion coefficients were determined for specimens diffused both with and without ultrasonics. The results indicate no enhancement for this system at the temperatures investigated, 550°K and 620°K. It is postulated that previously reported enhancement may have been due either solely to temperature increases caused by ultrasonic vibrations or enhanced grain boundary diffusion caused by the ultrasonic vibrations.

INTRODUCTION

The application of ultrasonic energy to industrial problems such as cleaning, non-destructuve testing, soldering, and welding is becoming quite wide spread today. The principles involved in such applications are basically simple and quite well understood. However, in recent years ultrasonics has been shown to have interesting effects on solid state metallurgical reactions such as carburization, precipitation hardening, etc. These effects have been demonstrated experimentally, but the principles are not well understood. Solid state diffusion is the basic reaction involved. Therefore, a direct investigation of diffusion should be most beneficial in promoting a better understanding of the effects of ultrasonics on all solid state reactions.

A review of the literature indicates a substantial increase in case depth during carburization by the use of ultrasonics.[1,2,3,4] Ultrasonics has also been shown to enhance precipitation hardening.[5] From these effects, it has been implied by these authors that ultrasonics enhances diffusion. In a recent study by Schoenthaler,[6] some doubt was placed on this implication. It is the objective of this study to further explore this area and attempt to clarify the conflicting results reported.

ANALYSIS OF PREVIOUS STUDIES

Schenck and Schmidtmann[1] reported a study of carburizing plain carbon steel under cyclic strain at 500 cycles per minute. They found that cyclic strain during carburizing increased the case depth achieved. This effect was found to increase with higher temperature and higher strain. They concluded from this that cyclic strain either enhanced diffusion or merely improved contact between the iron and the carburizing material. In further experiments they carburized without cyclic strain and then annealed with cyclic strain. A similar increase in case depth was noted. Thus, it was concluded that enhancement was not due merely to improved contact between iron and carburizing material. Following this they performed the same experiments using 450 kilocycles per second for the cyclic strain. The strain was less at this frequency but an even greater case depth resulted than at 500 cpm. Thus it was concluded that the total energy input, a factor of both frequency and intensity, was the factor influencing diffusion.

Rozanski[2] made similar conclusions from his study of carburization aided by ultrasonics. His main purpose was to study the simultaneous occurrence of graphitization with increased diffusion under ultrasonics, as Tanaka, et al.[3] had previously reported. Rozanski used 28 kcps for the exciting frequency and found that on excited samples, graphitization occurred at points of maximum stress and strain. The amounts of graphite decreased toward the point of minimum stress and strain as well as with lower temperatures. The unexcited samples showed no graphitization. Therefore, he concluded

that the increased rate of carbon diffusion with ultrasonics accelerated graphitization. Also, case depth was generally increased with ultrasonics.

Pogodin-Alekseev[4] verified the previous findings of increased case depth with ultrasonics being directly proportional to the stress amplitude. He suggested changes in the lattice parameters as the mechanism for this enhancement.

Gudtsov's findings reported by Ermakov and Al'ftan[5] showed that ultrasonics greatly reduced the time to obtain a fixed hardness through precipitation hardening of an alloy 78% Ni, 20% Cr and 1.4% Ti. It was also noted that this effect was independent of frequency between 300 cps and 1500 kcps, but dependent on intensity. Ermakov and Al'ftan[5] also reported similar results from a separate study of their own. They postulated that stressing the lattice increases the diffusion coefficient due to a decrease in the activation energy.

According to the analysis of Al'ftan,[7] strain or pressure is proportional to the product of frequency and amplitude while the rate of pressure change is proportional to the product of the square of the frequency times the amplitude. In a complete cycle the change in temperature of a unit volume of material varies directly with the rate of pressure change and inversely with the pressure. Diffusivity is proportional to this change in temperature. Thus, diffusivity is proportional to frequency.

$$D \sim \Delta T \sim \frac{\Delta P}{P} \sim \frac{f^2 A}{fA} = f$$

From this analysis, static strain will not accelerate diffusion in agreement with the work of Schenck and Schmidtmann.[1]

Balalaev[8] studied the effects of ultrasonic high temperature heating on the structure of technical iron. It was found that ultrasonic heating introduced points of active structural defects which increased the dissipation of energy during ultrasonic straining. This increase in temperature at the defects was sufficient to cause localized recrystallization at these points.

In a recent study by Schoenthaler,[6] the effects of ultrasonics on diffusion of copper in germanium were investigated. He concluded that diffusion was enhanced by the interstitial mode only. Since substitutional diffusion depends on vacancies in the germanium lattice, enhancement of this mode could only be effected by an increased vacancy concentration. Schoenthaler's work indicated consistent surface copper acceptor concentrations and concentration gradients with and without ultrasonics. It was deduced, therefore, that ultrasonics caused no increase in vacancy concentration and thus no enhancement of the substitutional mode of diffusion. However, the ultimate minimum level of acceptor concentration was increased by ultrasonics. Schoenthaler explains this as an enhanced interstitial mode of diffusion due to alteration of the crystal geometry during ultrasonic vibrations.

From Schoenthaler's study it is seen that what has previously been reported as enhanced diffusion may not necessarily be true. In view of this, it seems logical to conduct further experiments, highly controlled, aimed directly at measuring diffusion coefficients with the application of ultrasonic energy.

DESIGN OF EXPERIMENT

Detailed Procedures

To aid the reader in following the design of this experiment, detailed procedures and techniques have been eliminated from this section. The reader is referred to the following appendices for these details:

Appendix I - Plating Procedures

Appendix II - Diffusion Anneal

Appendix III - Sectioning and Counting

Appendix IV - Sample Calculations

Selection of Diffusion Couple

To best explore the area of doubt produced by Schoenthaler's work, substitutional diffusion was selected for study. From a practical standpoint a high rate of diffusion is desirable at reasonable operating temperatures. In addition to this, an accurate method of measuring the diffusion must be available. Radioactive tracer techniques are very accurate and well suited to self-diffusion which is strictly substitutional. Self-diffusion in most metals is of the order of 10^{-8} $cm^2/sec.$ at the melting point. Therefore, zinc was selected because of its relatively low melting point, $693^{o}K$, and a readily available radioactive isotope, Zn^{65}.

Zinc Specimens

Zinc has a hexagonal close packed structure with a c/a axial ratio of 1.86. Consequently, an anisotropy of diffusivity exists in zinc.

This anisotropy is reported in several studies of self-diffusion in zinc.[9,10] Therefore, in addition to using single crystals to eliminate grain boundary effects, the single crystals were oriented so as to independently study diffusion both parallel and perpendicular to the c axis. As shown in Appendix II, the specimens must be cut to a length equal to 0.58 times the resonant wavelength. This wavelength was determined by the relationships given by Mason:[11]

$$\lambda \text{ (// c axis)} = \frac{V \text{ (// c axis)}}{f} = \frac{\sqrt{c_{33}/\rho}}{f}$$

$$\lambda \text{ (// basal plane)} = \frac{V \text{ (// basal plane)}}{f} = \frac{\sqrt{c_{11}/\rho}}{f}$$

where λ is the wavelength, V is the velocity of sound, ρ is the density of zinc (7.1 gms./cc) and f is the driving frequency, 58.5 kcps for this experiment. The constants c_{33} and c_{11} are given by Mason as being 5.31×10^{11} dynes/cm^2 and 16.35×10^{11} dynes/cm^2, respectively. The calculated resonant wavelengths for zinc are:

$$\lambda \text{ (// c axis)} = 1.84 \text{ in.}$$

$$\lambda \text{ (// basal plane)} = 3.23 \text{ in.}$$

and the calculated specimen lengths are:

$$0.58\,\lambda \text{ (// c axis)} = 1.067 \text{ in.}$$

$$0.58\,\lambda \text{ (// basal plane)} = 1.875 \text{ in.}$$

Therefore, for diffusion parallel to the c axis, the specimens were parallelepipeds 0.250" square by 1.9" long with the basal plane parallel to one of the 0.250" by 1.9" faces. The direction of ultrasonic motion in this case was parallel to the basal plane. For diffusion parallel

to the basal plane, the specimens were parallelepipeds 0.250" square by 1.1" long with basal plane parallel to the 0.250" by 0.250" end faces. The direction of ultrasonic motion in this case was parallel to the c axis.

Experimental Procedures

Specimens of the required dimensions and orientation were purchased from Leytess Metal and Chemical Corporation. The specimen purity was 99.999%. The radioactive tracers, Zn^{65}, were obtained from Tracerlabs, Inc. in small glass vials containing ten microcuries each in the form of $ZnCl_2$ dissolved in a half normal HCl solution.

The radioactive tracers were deposited on the diffusion surface of the specimen by electroplating as outlined in Appendix I. The specimen was then placed in the diffusion furnace and heated to the diffusion temperature. Great care was taken to obtain true specimen temperatures. As indicated in Appendix II this was accomplished by using separate thermocouple leads, individually held in contact with the specimen. Thus, accurate specimen temperatures were obtained, since only when both leads were in contact with the specimen was any reading obtained. This was necessary in view of the exponential effect of temperature on diffusion rate. Specimens of each orientation were diffusion annealed at the same temperature both with and without ultrasonics to obtain an accurate comparison of diffusion coefficients with and without ultrasonics. After the diffusion anneal, the center half inch was cut from the specimen for sectioning and counting as detailed in Appendix III. A mechanical lapper was

used for sectioning. Radioactive counts were made on the material removed from the specimen. Each sectioning operation lapped to a depth of approximately thirteen microns, and from nine to twelve sections were made on each specimen. An example of the calculations involved is given in Appendix IV. The counts recorded on the individual sections decreased approximately one order of magnitude from the surface to the final section taken on each specimen. Shewmon[12] and Crank[13] have developed a thin film solution for accurate determination of diffusivity of substitutional atoms according to the following relationship:

$$\frac{d \ln c(x,t)}{d (X^2)} = -\frac{1}{4 Dt} = \text{slope}.$$

From this relationship, D, the diffusion coefficient, can be calculated from the slope of a plot of the natural logarithm of concentration (c) versus the square of the penetration distance (X) for a given time (t). Since the number of counts, or activity (A), of the species is directly proportional to the concentration of the species, the natural logarithm of activity may be substituted into the above relationship giving:

$$\frac{d \ln A}{d (X^2)} = -\frac{1}{4 Dt} = \text{slope}$$

or

$$D = -\frac{1}{4t(\text{slope})}.$$

The data for activity (A) and penetration depth (X) obtained from the sectioning and counting were analyzed by a simple step-wise linear

regression computer program to obtain the best slope of a plot of ln A versus X^2. D was then calculated from the computer value for the slope and known diffusion time.

RESULTS

The results of the experiments performed are summarized in Table 1. The results of specimens 1 through 7 are of little value other than an indication that better temperature sensing was needed. It is not known exactly what temperature was measured for these specimens, since the readings varied depending on the intimacy of contact between the welded thermocouple leads and the specimen. Therefore, there is a wide variation in the results, in addition to a large deviation from the results predicted using previously published figures.[9]

For the remaining specimens, the thermocouple was modified as indicated in Appendix II to insure true specimen temperature readings.

The diffusion coefficients listed in Table 1 were obtained from the slope of a plot of the natural log of activity versus the square of the mean penetration distance. Predicted ranges for the diffusion coefficients were obtained using the empirical equations of Miller and Banks.[9]

$$D\ (//c\ \text{axis}) = 0.046 \exp \frac{-20{,}400 \pm 900}{RT}$$

$$D\ (//\text{basal plane}) = 92 \exp \frac{-31{,}000 \pm 3000}{RT}$$

It can be seen in Table 1 that all the experimental diffusion coefficients, using the modified temperature measurement (specimens 8 through 22), are well within the predicted ranges. In addition to this the results obtained with ultrasonics overlap those without ultrasonics.

Specimens 13 and 14 were heated to 620°K without ultrasonics. Once the power setting for the furnace was established to maintain this temperature, ultrasonic energy was applied. An immediate temperature increase was noted, and after approximately ten minutes the temperature was stable once more, but at the indicated higher values. Thus, the ultrasonic energy used in these experiments resulted in an 8° to 13°C rise in temperature.

Plots of the natural logarithm of activity versus the square of the mean penetration distance for all specimens are contained in Appendix III. The slope of such a plot is proportional to the product of the diffusion coefficient times the diffusion time. Since diffusion times and surface activity varied from specimen to specimen, a graphical comparison of the diffusion coefficients can be obtained from plots, normalized with respect to surface activity and diffusion time. Normalized plots for the three temperature-orientation conditions are shown in Figures 1, 2, and 3. Again in these plots it can be seen that the results of these experiments are well within the predicted ranges. The overlap of results with and without ultrasonics is also evident in these plots.

TABLE 1

Summary of Experimental Results

Specimen	Ultrasonics*	Time	D(cm^2/sec.)
		Diffusion // c axis @ 610°K**	
1	No	1.5 hr.	5.07×10^{-10}
2	No	5.0 hr.	3.13×10^{-10}
3	No	"	4.24×10^{-10}
4	No	"	2.77×10^{-10}
5	Yes	"	1.93×10^{-10}
6	Yes	"	3.52×10^{-10}
7	Yes	"	3.71×10^{-10}
Predicted Range		-	11.6×10^{-10} to 51.6×10^{-10}
		Diffusion // basal plane @ 620°K	
8	No	4.0 hr.	1.59×10^{-9}
9	No	3.0 hr.	1.91×10^{-9}
10	No	"	1.35×10^{-9}
11	Yes	"	1.37×10^{-9}
12	Yes	"	1.47×10^{-9}
Predicted Range		-	1.16×10^{-10} to 1.39×10^{-8}
		Diffusion // c axis @ 620°K	
15	No	80 min.	2.66×10^{-9}
16	No	90 min.	3.72×10^{-9}
17	Yes	"	3.75×10^{-9}
18	Yes	"	2.89×10^{-9}
Predicted Range		-	1.83×10^{-9} to 6.66×10^{-9}
		Diffusion // c axis @ 550°K	
19	No	7.25 hr.	4.11×10^{-10}
20	No	"	2.92×10^{-10}
21	Yes	"	3.57×10^{-10}
22	Yes	"	2.18×10^{-10}
Predicted Range		-	2.10×10^{-10} to 8.98×10^{-10}

Diffusion // basal plane (ultrasonic heating effect)

Specimen	Temp. (no u/s)	Temp. (with u/s)	D(cm^2/sec.)
13***	620°K	628°K	2.13×10^{-9}
14***	620°K	633°K	2.57×10^{-9}

* In all cases the direction of ultrasonic motion was perpendicular to the direction of diffusion.

** 610°K was recorded temperature. Actual specimen temperature was unknown.

*** Specimens 13 and 14 were brought to 620°K without ultrasonics. Ultrasonic energy was then applied while the power input to the diffusion furnace was maintained constant.

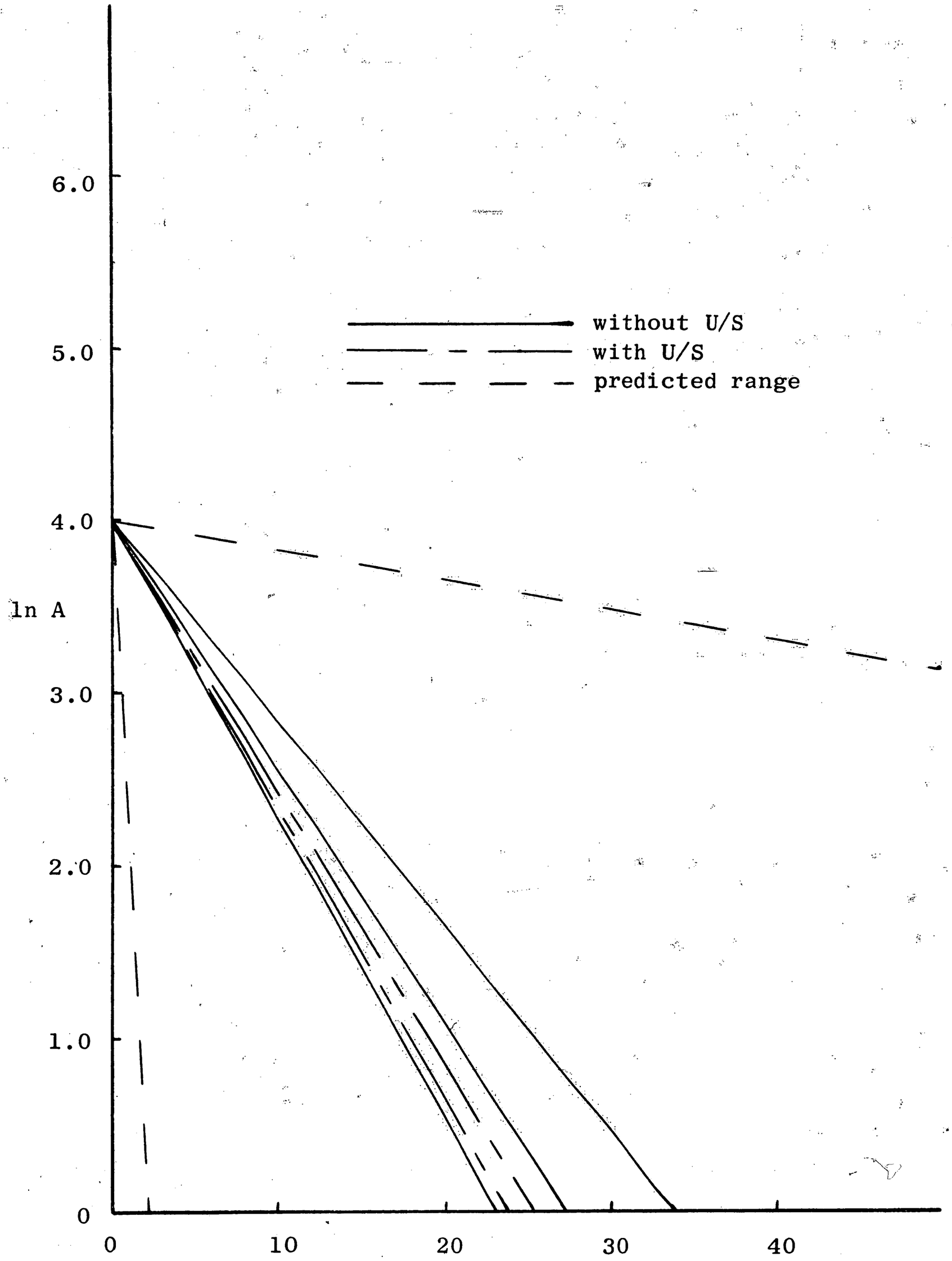

FIGURE 1

Normalized plot of natural logarithm of Activity versus square of mean penetration distance for specimens diffused // basal plane at $620^{o}K$.

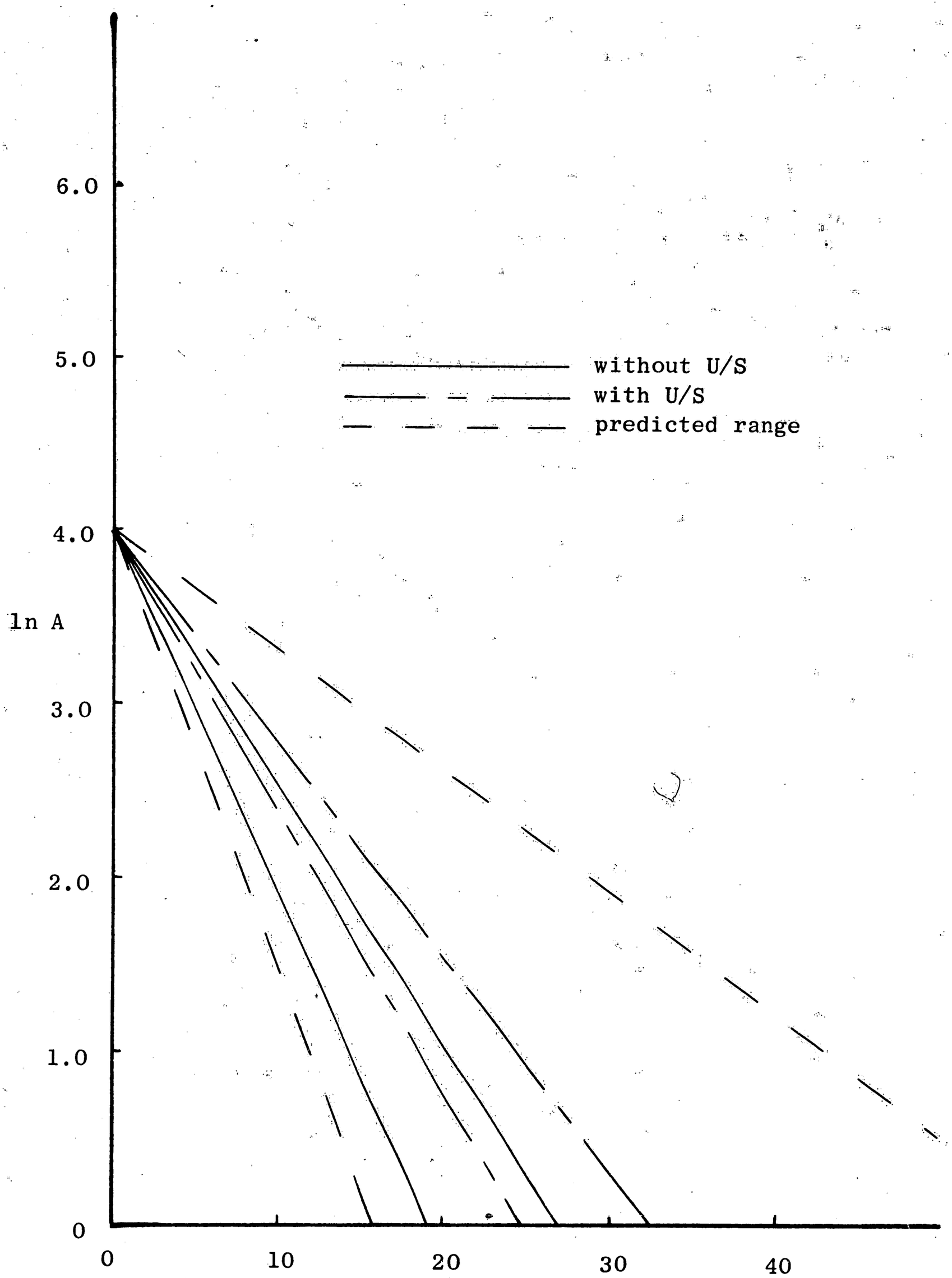

FIGURE 2

Normalized plot of natural logarithm of Activity versus square of mean penetration distance for specimens diffused // c axis at 620°K.

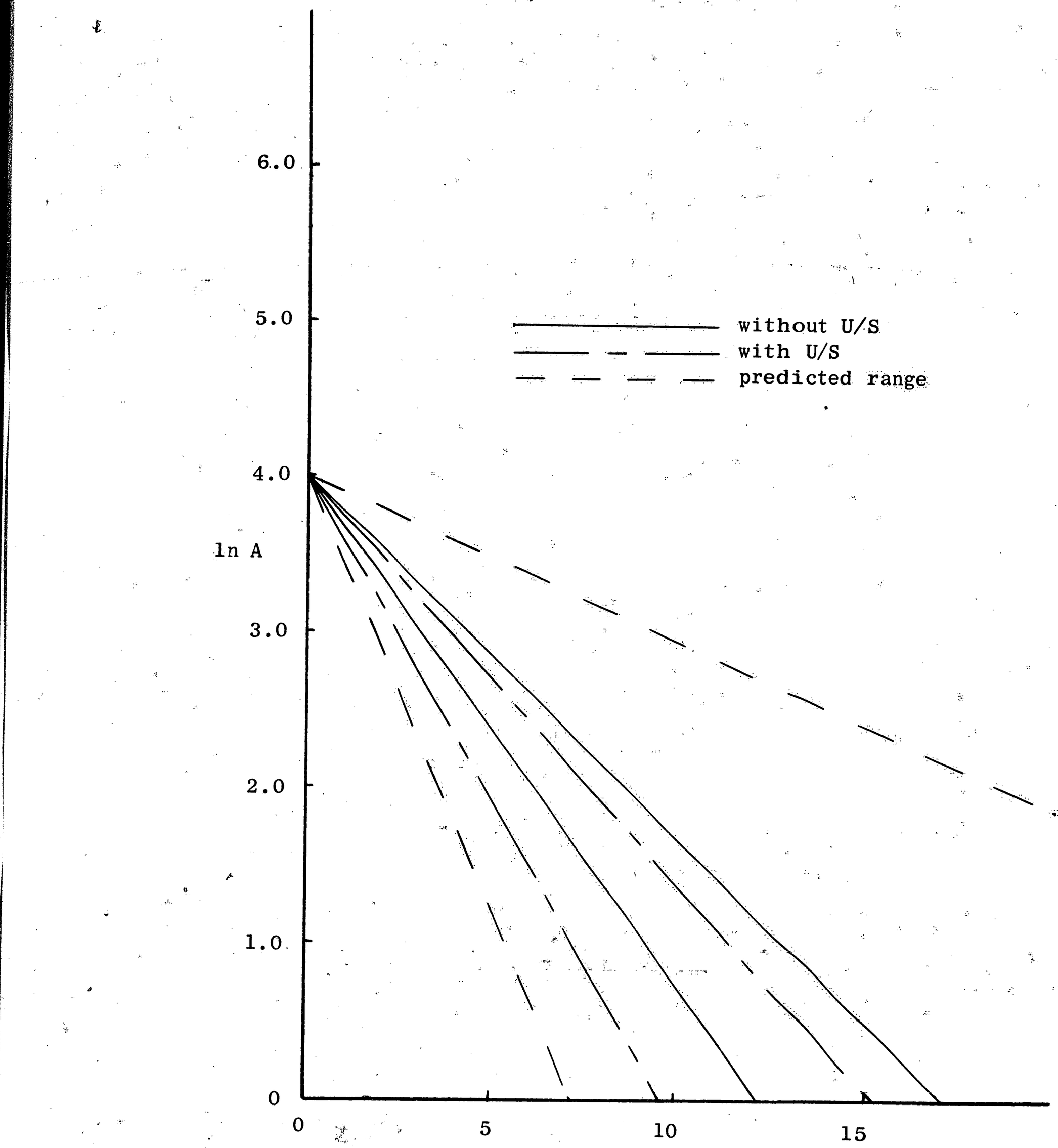

FIGURE 3

Normalized plot of natural logarithm of Activity versus square of mean penetration distance for specimens diffused // c axis at 550°K.

DISCUSSION

For comparison of results, it would be best to categorize all the systems studied as to the probable mode of diffusion. Carburization in the iron-carbon system most probably involves interstitial diffusion. Precipitation hardening in the nickel-chromium-titanium system most probably involves substitutional diffusion. The diffusion of copper in germanium reportedly involves a combination of interstitial and substitutional diffusion. The zinc self-diffusion is most probably substitutional diffusion. In addition to this, the presence of grain boundary diffusion must be considered for polycrystalline materials.

Consider, first, the case of substitutional diffusion. The results of the present zinc self-diffusion study are in basic agreement with the copper-germanium study,[6] in that substitutional diffusion was not enhanced by ultrasonics. The precipitation hardening study by Ermakov and Al'ftan[5] indicated enhanced substitutional diffusion. The lack of detail in this study makes it difficult to analyze. However, in the experimental setup, the thermocouple did not appear to be in contact with the specimen. If this was the case, true specimen temperatures would not be obtained. In fact, as evidenced by the first seven specimens in the present zinc study, simple contact of welded thermocouple leads with the specimen is not sufficient for accurate temperature control. Therefore, ultrasonic heating may not have been detected by Ermakov and Al'ftan. In analyzing the data in their report, it appears that the application of ultrasonic energy gave approximately the same increase in aging as might be given by a

temperature rise of approximately 50-70°C. The ultrasonic generator used in their experiment was rated at 800 watts output, however no indication is given as to the power used or the specimen size in the experiment. With such high powers available, the 50-70°C temperature rise does not seem unreasonable, in view of the 8-13°C rise achieved in zinc with the application of approximately 1.6 kilowatts per square inch of cross-section and in view of Balalaev's[8] report that iron was recrystallized by ultrasonic heating, a temperature rise of approximately 900°C (the ultrasonic power used in this study is not indicated in the report). Since this present study and that of Balalaev indicates that ultrasonics can have considerable heating effect, it seems feasible that ultrasonic heating could have been the cause of the increased precipitation rates reported by Ermakov and Al'ftan.

Another factor to be considered in the precipitation hardening study is grain boundary diffusion, since the specimens used were polycrystalline. It is possible that ultrasonic vibrations may have some geometry effect on the grain boundary areas making them higher diffusivity paths or "pipes" for increased mass transport. Schoenthaler's[6] copper-germanium study and the present zinc self-diffusion study involved no grain boundary diffusion since single crystal specimens were used.

Consider, now, the interstitial mode of diffusion. No direct comparison can be made between substitutional diffusion in this zinc study and the interstitial diffusion in previous carburization studies or interstitial diffusion in the copper-germanium system. However, extension of the ultrasonic heating analysis to interstitial diffusion

may have some merit. The studies of Schenck and Schmidtmann[1] and Rozanski[2] indicate that carburizing with ultrasonics increased the case depth achieved by a factor of 1.5 to 2.0. Solutions to Fick's second law show that the diffusion coefficient, D, is proportional to the square of the depth of penetration. Therefore, a twofold increase in case depth would result from a fourfold increase in D. For the iron-carbon system, at the temperatures used by Schenck and Schmidtmann[1] and Rozanski,[2] 900°C, an increase of 150°C would result in a fourfold increase in D. The ultrasonic power used by Schenck and Schmidtmann was approximately 1.75 kilowatts per square inch of cross-section. The ultrasonic power used by Rozanski varied from approximately 3.7 to 12.4 kilowatts per square inch of cross-section. In view of this, ultrasonic heating cannot be ruled out as a possible cause of the reported interstitial enhancement.

In addition to this, all of the carburization studies have involved polycrystalline materials, so that the effect on grain boundary diffusion is also possible as in the case of the substitutional studies.

Still another possibility has been suggested for enhanced interstitial diffusion. Schoenthaler[6] has suggested that ultrasonic energy enhances interstitial diffusion by altering the lattice parameters of the crystal structure. This is described by Schoenthaler as a geometric and probability effect reducing the energy difference between an occupied site and the saddle point through which the atom must move to reach an adjacent unoccupied site, thereby causing an increase in the jump frequency. This is similar to the suggested grain boundary enhancement except that it affects interstitial diffusion within the crystal lattice..

SUMMARY

It was the objective of this study to help clarify conflicting results reported on ultrasonic enhancement of diffusion. Direct measurements of self-diffusion coefficients for zinc were made using radioactive tracer techniques. The results of this study have been analyzed along with previous results and the conclusions drawn are summarized as follows:

1. Ultrasonics has no effect on self-diffusion in single crystalline zinc, either parallel or perpendicular to the c axis, within the temperature range of 550°K to 620°K with the exciting frequency of 58.5 kcps.
2. It is suggested that previously reported enhancement in probable substitutional diffusion systems may have been due to ultrasonic heating or enhanced grain boundary diffusion by some effect. Obtaining true specimen temperature is essential to detect the ultrasonic heating effect and in the one case of reported enhanced substitutional diffusion, a temperature increase of 50-70°C would account for the reported enhancement. Grain boundary diffusion was present in the one case of enhancement and was not present in the two cases where no enhancement was reported.
3. For the case of probable interstitial diffusion no direct comparison can be made with the present zinc self-diffusion study. However, the possibility of

ultrasonic heating and enhanced grain boundary diffusion cannot be ruled out. Schoenthaler's suggested geometric and probability enhancement of interstitial diffusion is also consistent with reported results.

APPENDIX I

Plating Procedures

Specimen Preparation

The specimens received from the supplier were cut and lapped to size. In attempting to verify the orientation of the crystals by back reflection Laue X-ray photographs it was discovered that the specimens had a surface layer of either polycrystalline and/or highly strained crystal structure. It was therefore necessary to remove this layer so that the Zn^{65} could be plated directly on a single crystal surface. This was accomplished by hand lapping the surface to be plated with 600 grit wet lapping paper. The specimen was then etched in a solution of 15% concentrated HCl in alcohol for approximately one hour. Back reflection Laue X-ray photographs were then made of several of the specimens to insure that the exposed surface was single crystalline.

Plating Solution

The plating bath used to deposit the Zn^{65} on the specimen consisted of:

20 ml. H_2O

0.5gm. $ZnCl_2$

0.3gm. NH_4Cl

The Zn^{65} was received from the supplier in small vials containing ten microcuries each in a half normal solution of HCl. The isotope was introduced into the bath by rinsing the vial with the prepared

plating solution. By the use of a survey meter it was determined that approximately 95% of the Zn^{65} was transferred to the plating bath by this rinsing.

Plating Apparatus

The plating apparatus is shown in schematic in Figure I-1. The plating tank was a small plastic box approximately 3" x 2" and 1.5" deep. A sheet carbon anode was glued to the inner bottom surface of the tank. The specimen, acting as the cathode, was suspended over the carbon anode so that the plating surface contacted the solution by surface tension. Nitrogen was bubbled into the bath to prevent the buildup of bubbles on the plating surface. A DC power supply and milliammeter in series with the tank completed the setup.

Procedures

From preliminary experiments it was determined that a current density of approximately 110 ma/in.^{2} would give good adherence and even plating over the entire surface with the above mentioned solution. A plating curve, as shown in Figure I-2, was determined for the bath and current density mentioned using a surface area of 1.9 in.^{2} (equivalent to the plating surface of four specimens 1.9 in. long). It was possible to plate out approximately 85% of the zinc in solution in 90 minutes. The fact that Zn^{65} plated out at the same rate as indicated by the plating curve was verified by survey meter readings of the plating solution before and after plating. The solution activity after plating was approximately 20% of the solution activity before

plating. Four specimens were plated simulaneously. Since the bath initially contained nine to ten microcuries of Zn^{65}, approximately eight microcuries were deposited on the four specimens, or two microcuries per specimen. After plating, the four faces surrounding the plated surface of each specimen were hand lapped on 600 grit paper to remove all traces of Zn^{65} from all but the diffusion surface. At this point the specimen was ready for the diffusion anneal.

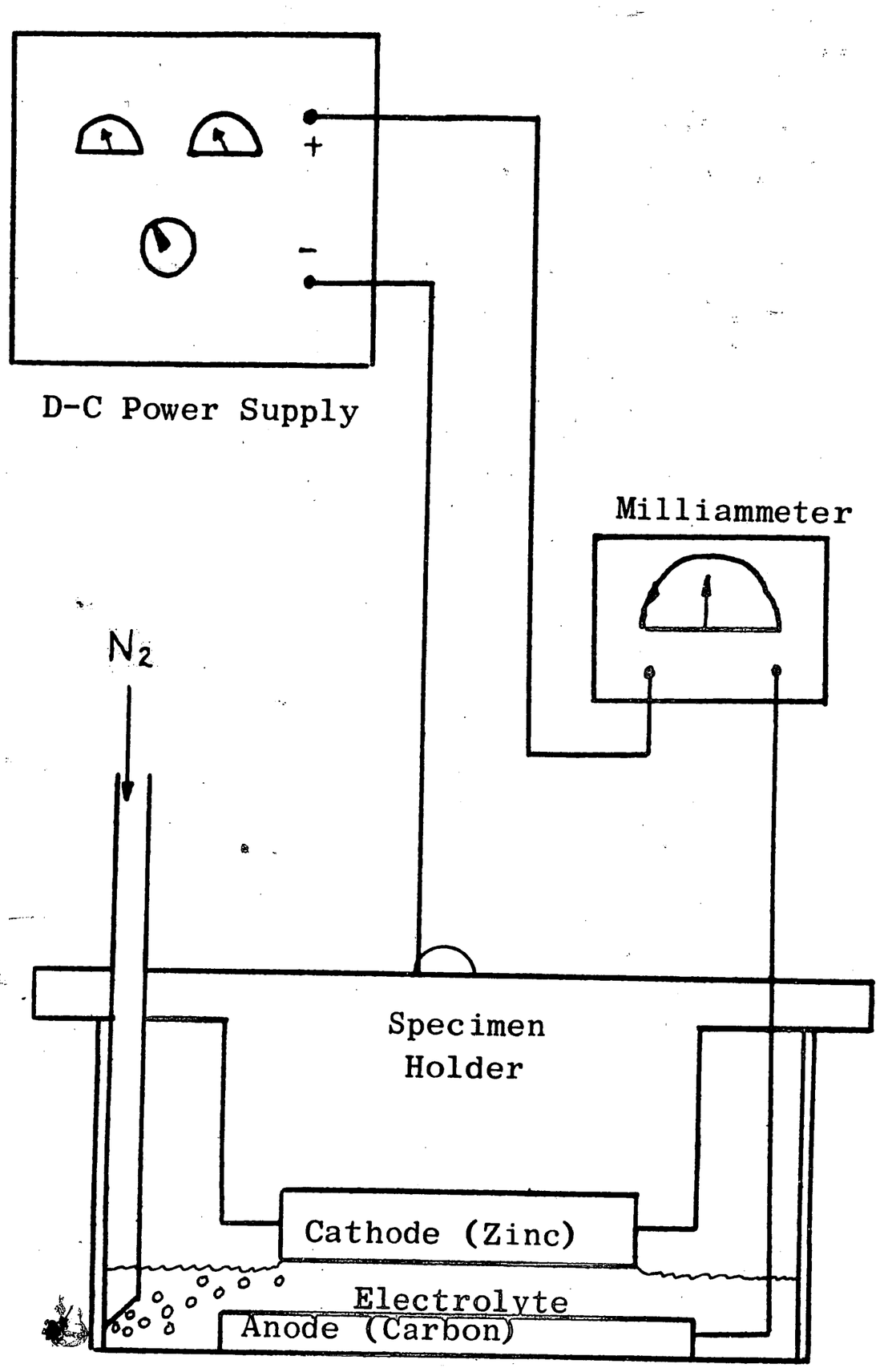

PLATING TANK

FIGURE I-1

Schematic Illustration of Plating Apparatus

Plating Bath Initially Contained 240 mg. of Zinc in Solution.

TIME(min.)	SPEC.WT.(mg)	Δ WT.(mg)	Σ Δ WT.(mg)	% PLATED
START	124203.5			
30	124322.9	119.4	119.4	49.5
60	124389.2	66.3	185.7	77.1
90	124411.5	22.3	208.0	86.3
110	124416.4	4.9	212.9	88.4

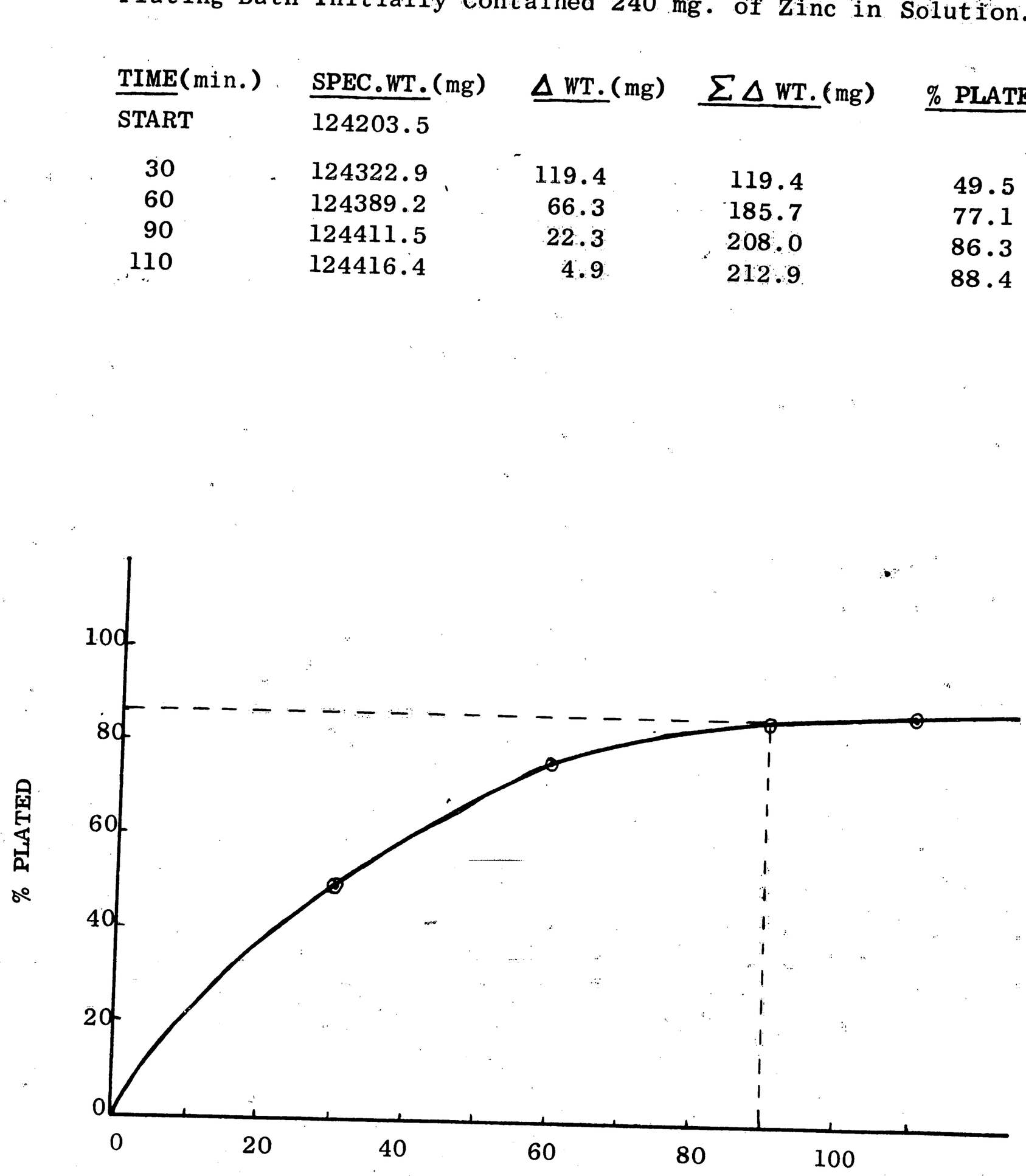

FIGURE I-2

Plot of % of total zinc in solution plated versus plating time.

APPENDIX II

Diffusion Anneal

Ultrasonic System

The ultrasonic system used for this study is shown schematically in Figure II-1. This system requires no metallurgical joining of the specimen to the acoustical transmission line since the 58.5 kcps ultrasonic driver shown as part (1) and the followup section (2) clamp the specimen (3) in position by means of the constant pressure air cylinder (5). This pressure was maintained at 165 psi. This stress caused varying degrees of deformation of the specimens depending on the crystal orientation and diffusion temperature. Stress perpendicular to the c axis of the crystal generally caused more deformation than did stress parallel to the c axis of the crystal. Higher temperature also increased the resulting deformation. In all cases the deformation was concentrated in either end of the specimen and the center half of the specimen exhibited no measurable deformation. The specimens diffused at 550^{o}C exhibited no measurable deformation throughout their length.

The ultrasonic driver and followup section made of titanium pieces were four inches in length from clamping point to the end in contact with the specimen. Using the relationship given by Mason,[11] $\lambda = V/f$, the resonant wavelength, λ, in titanium is calculated to be 3.3 inches at frequency, f, of 58.5 kcps, taking velocity of sound in titanium, V, as 1.95×10^5 in./sec. The four inch driver and followup section, therefore, are each 4.0/3.3 = 1.21 times the resonant wavelength.

Clamping pressure must be applied at stress nodes of the transmission line in order to preserve resonance. Therefore, a specimen length of 0.58 times the resonant wavelength in zinc, will place the clamping pressure application points at stress nodes exactly three wavelengths apart, with the specimen spanning slightly more than half a wavelength. A soft iron segment (4), attached to the titanium followup section (2) supports the magnetic field of the permanent magnet incorporated in the amplitude detector. The magnetic flux passing through a variable air gap permits measurement of the excursion of the end member by a commercial Hall cell, the output of which was monitored on an oscilloscope. The ultrasonic system was maintained at resonance by varying the frequency slightly to maintain the signal at maximum amplitude.

Diffusion Furnace

Again referring to Figure II-1, the furnace moves vertically to position the specimen in the center of a circular array of six Globars, the heating elements in the furnace. The cooling heat exchangers were used to cool the driver probe and followup section and prevent overheating the ultrasonic transducer. A split cylindrical stainless steel chamber was placed around the specimen. This chamber was purged with a dynamic argon atmosphere (4 ft.^{3}/hr.) to prevent oxidation during the anneal. An iron-constantan thermocouple was inserted in a small opening in the top of the chamber to obtain temperature readings on the zinc specimen. For specimens 1 through 7, the thermocouple leads were welded together and the couple then placed in contact with the zinc surface. It was then discovered that this arrangement did

not give true specimen temperature, since the readings varied depending on the intimacy of contact between the thermocouple and specimen. This problem was then corrected by using separate thermocouple leads and cutting them to sharp points. The two leads were separately held in contact with the specimen. Thus, accurate specimen temperature readings were obtained, since only when both points touched the specimen was any reading obtained.

Procedures

The specimen was clamped in place and the chamber atmosphere adjusted by purging with argon at four cubic feet per hour. The furnace was then lowered over the specimen and atmosphere chamber. Power was supplied to the furnace through a variac. The specimen was brought to temperature by manually adjusting the output of the variac. With the proper power settings it was possible to reach operating temperature with little or no overshoot in nine minutes. The voltage input to the furnace and specimen temperature were monitored throughout the anneal. The temperature was maintained constant, plus or minus two degrees Kelvin, with minor voltage corrections of less than one volt.

After the appropriate diffusion time, it took approximately two minutes to raise the furnace, remove the atmosphere chamber, and quench the specimen in water.

Effective Diffusion Time

Shewmon[12] outlines a simple method for determining an effective diffusion time, t', to compensate for heatup and cooling times. This can be determined graphically from a plot of D, diffusion coefficient,

versus t, diffusion time. First, a plot of T temperature, versus time is made. This plot is then transformed to a plot of D versus time using the Arrhenius equation, $D = D_o \exp \frac{-Q}{RT}$. For ease in plotting, T/T' and D(T)/D(T') are used, where T' is the effective diffusion temperature, 620°K or 550°K, as the case may be. Typical data and plots are shown in Figure II-2. It can be seen in this figure that the time spent in heating to approximately 0.8 T' contributes nothing to the total diffusion. By arbitrarily setting the end of effective diffusion time at the beginning of cooling, t' is determined by equating crosshatched areas within t' to crosshatched areas outside t'. This results in effective diffusion time beginning at six minutes after the start of heating.

1 - 58.5 KCPS U/S Driver
2 - Back-Up Section
3 - Zinc Specimen
4 - Hall Cell
5 - Constant Press.-Force
6 - Horizontal Slide

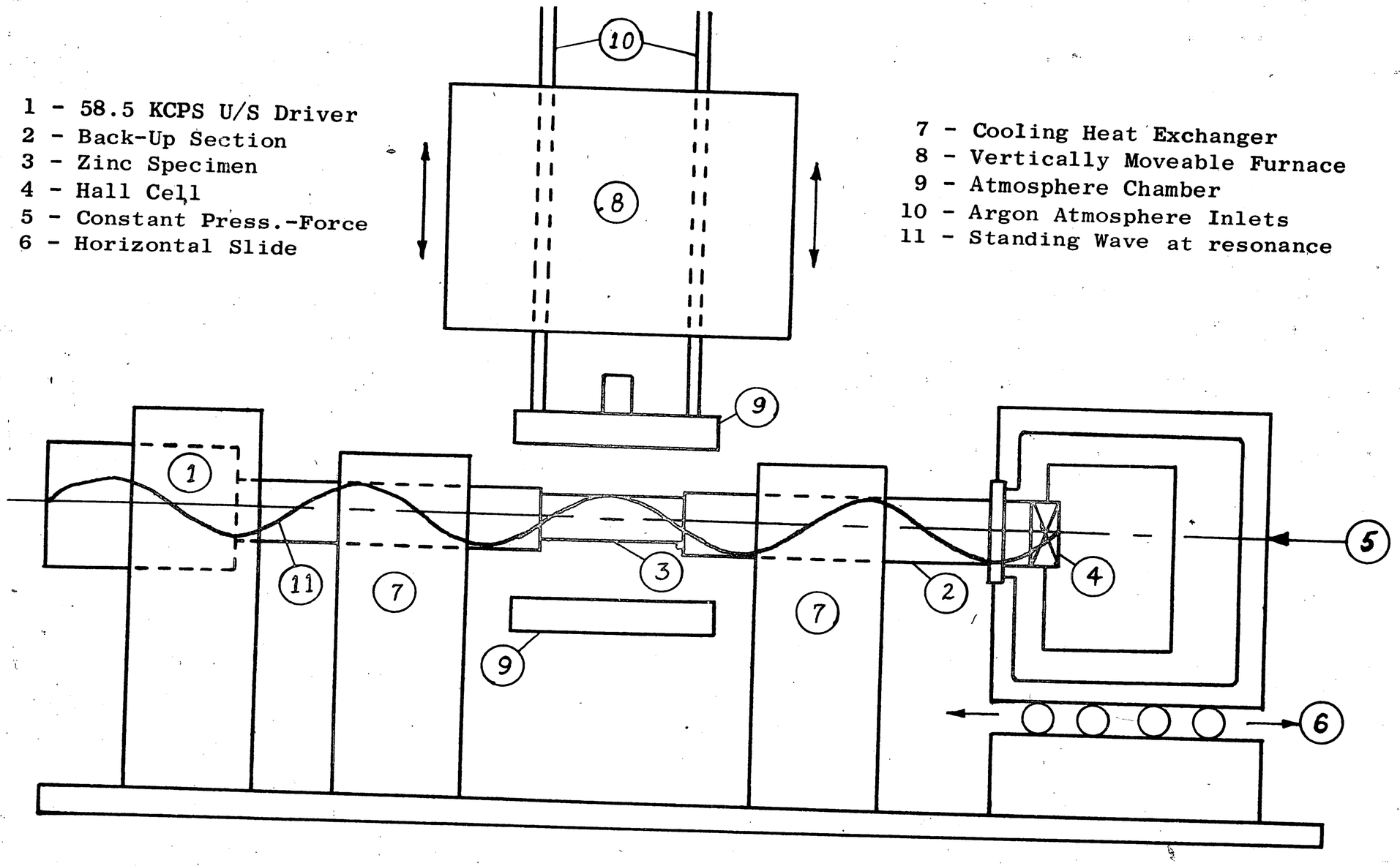

7 - Cooling Heat Exchanger
8 - Vertically Moveable Furnace
9 - Atmosphere Chamber
10 - Argon Atmosphere Inlets
11 - Standing Wave at resonance

FIGURE II-1

Schematic Illustration of Ultrasonic Diffusion Equipment

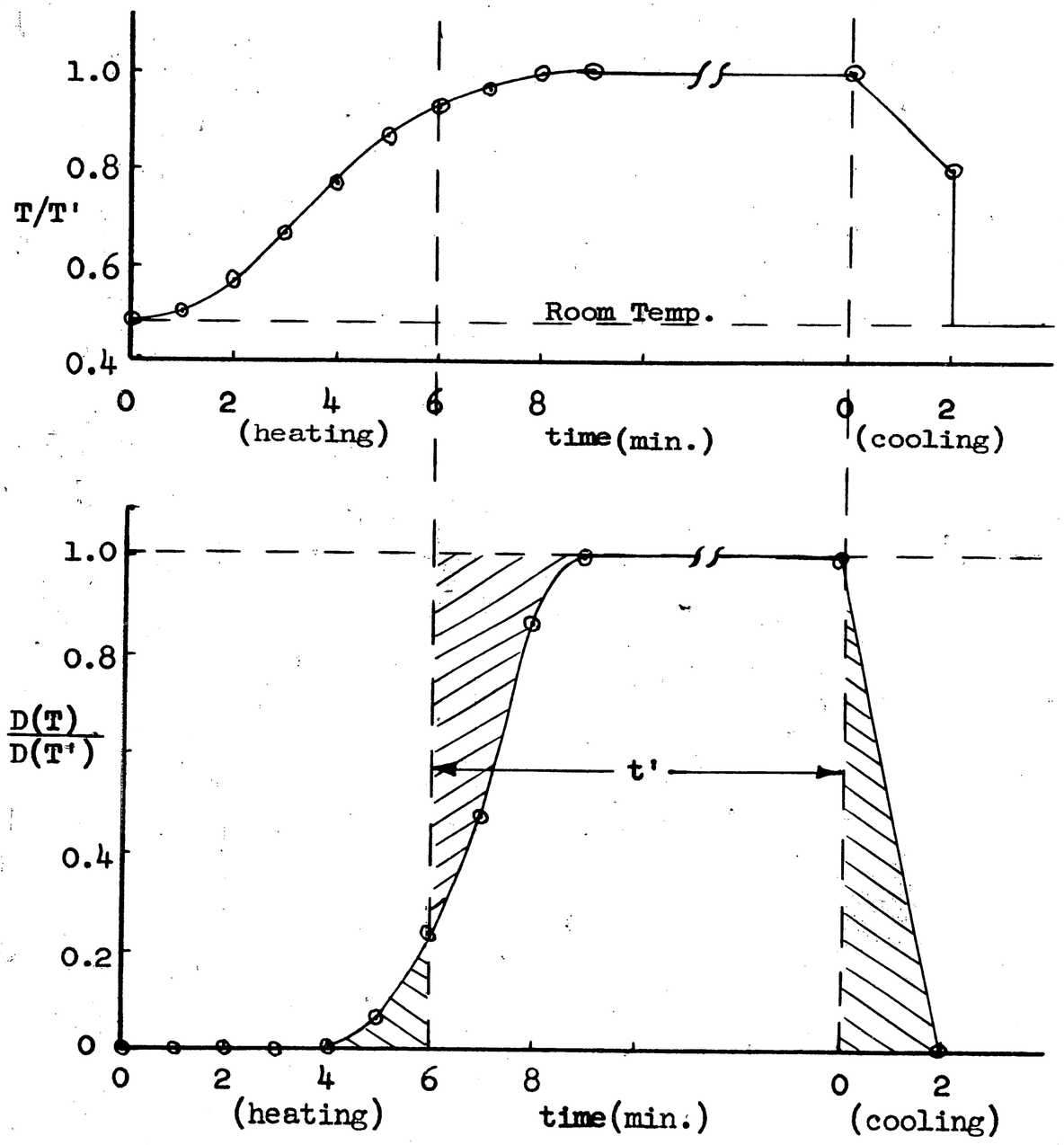

Heating

Time(min.)	T(°K)	T/T'	D(T)/D(T')
0	300	.483	~ 0
1	314	.506	~ 0
2	353	.569	~ 0
3	409	.660	~ 0
4	475	.766	~ 0
5	533	.860	0.068
6	572	.922	0.251
7	594	.958	0.478
8	616	.993	0.870
9	620	1.000	1.000

Cooling

Time(min.)	T(°K)	T/T'	D(T)/D(T')
0	620	1.000	1.000
2	500	.806	~ 0

FIGURE II-2

Determination of effective diffusion time, t', at effective diffusion temperature, T'

APPENDIX III

Sectioning and Counting

Specimen Preparation

After the diffusion anneal, the center half inch of length was cut from the specimen. To avoid excessive slip at the cutting surface, a special vise was designed which clamped the specimen securely on either side of the cutting line. The surfaces perpendicular to the diffusion surface were then hand lapped on 600 grit lapping paper, removing approximately five mils from each surface. This was done to eliminate the effect of surface diffusion. The area of the diffusion surface was then measured and recorded.

Sectioning

The specimen was mounted in a mechanical lapping machine for sectioning. Wet lapping on 600 grit paper was used to remove thin layers of zinc from the diffusion surface. Through preliminary experiments it was determined that the mechanical lapper produced a surface, flat within four microns over the half inch length, and within one micron over the middle quarter inch. The specimen was weighed to the nearest tenth of a milligram before and after each lapping sequence to determine the weight of zinc removed. From this weight loss, the density of zinc (7.1 gm./cc), and the measured surface area, the depth of sectioning was calculated. Most of the material lapped from the specimen remained on the wet lapping paper. The specimen was rinsed onto the lapping paper each time with several drops of water and then wiped clean with a small piece of tissue to remove any

particles clinging to the specimen. In this manner all visible traces of lapped material were removed from the specimen and deposited on the lapping paper.

Counting

The activity of the lapped material was then determined using a scintillation counter. The amplifier and pulse height analyzer were adjusted to count gamma radiation from a Zn^{65} standard source. The counter was preset to record the time required for five thousand counts. From this, a counts per minute figure was determined for each section. The level of unavoidable background radiation was determined prior to and several times between sections on each specimen. The CPM figure for each section was corrected by subtracting the background radiation (in cpm). Since the depth of sectioning varied with each section, the above corrected figure was standardized by calculating cpm per unit of depth. The counting error ranged from approximately 1% near the surface to approximately 2% at the deepest point. These figures were determined using the following relationship given by Cullity:[14]

$$\%E = \frac{67\ \sqrt{N + N_B}}{N - N_B}$$

where N = the total number of counts counted

N_B = the total number of background counts

Determination of D

A plot of the natural logarithm of activity (ln A), versus the square of the mean penetration distance (X^2) was made. X is the distance from the original diffusion surface to the center of the

section in question. Values of X and A were analyzed by a simple step-wise regression computer program to find the best slope to this plot. From the thin film solution to Fick's second law, the slope of this plot is equal to $-\frac{1}{4t(\text{slope})}$, where D is the diffusion coefficient and t is the diffusion time. Thus the diffusion coefficient is given by

$$D = -\frac{1}{4t(\text{slope})} .$$

Plots of the natural logarithm of activity versus the square of the mean penetration distance for the various conditions investigated are shown in Figures III-1 through III-6.

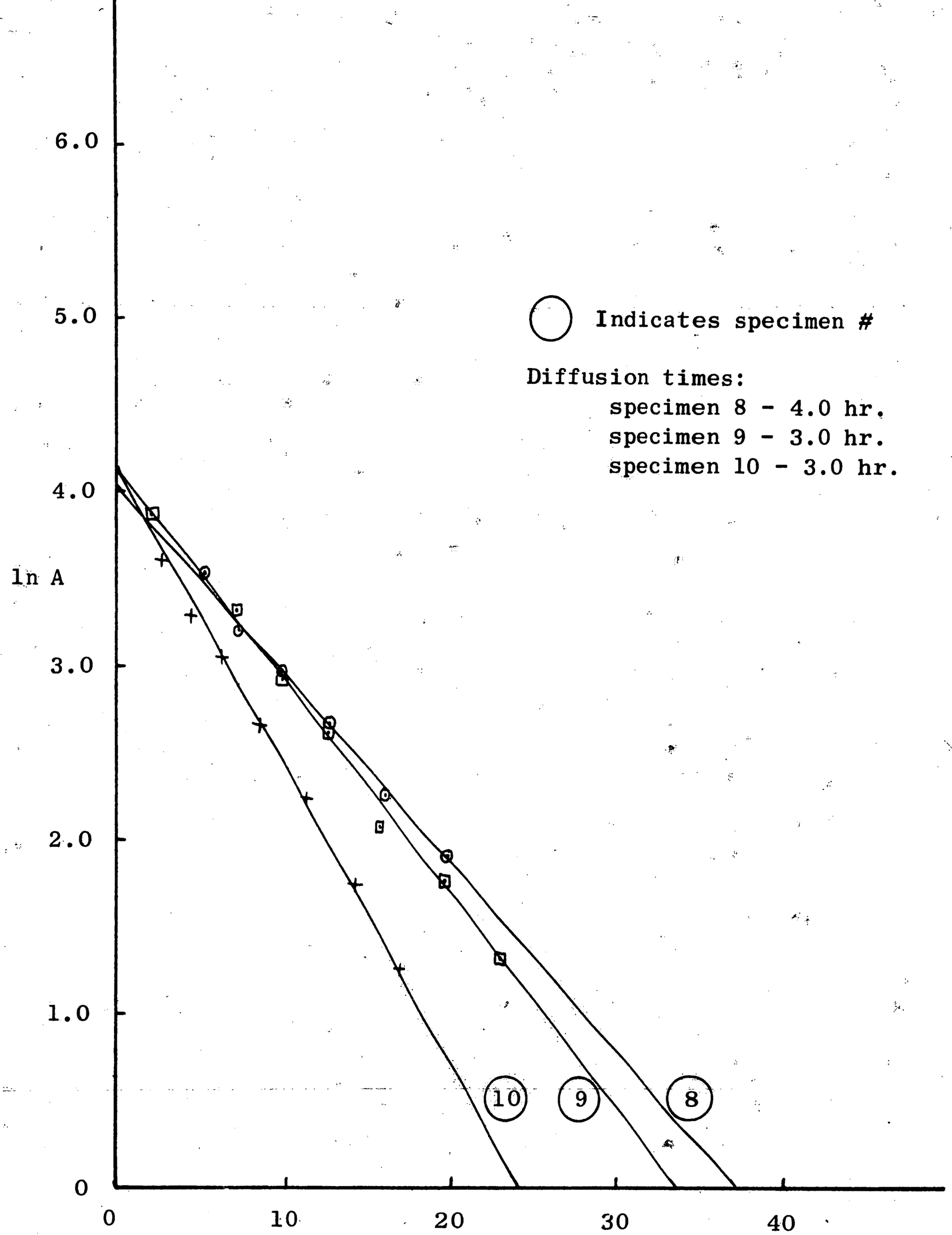

◯ Indicates specimen #

Diffusion times:
specimen 8 - 4.0 hr.
specimen 9 - 3.0 hr.
specimen 10 - 3.0 hr.

FIGURE III-1

Plot of natural logarithm of Activity versus square of mean penetration distance for specimens diffused // basal plane at 620°K without ultrasonics.

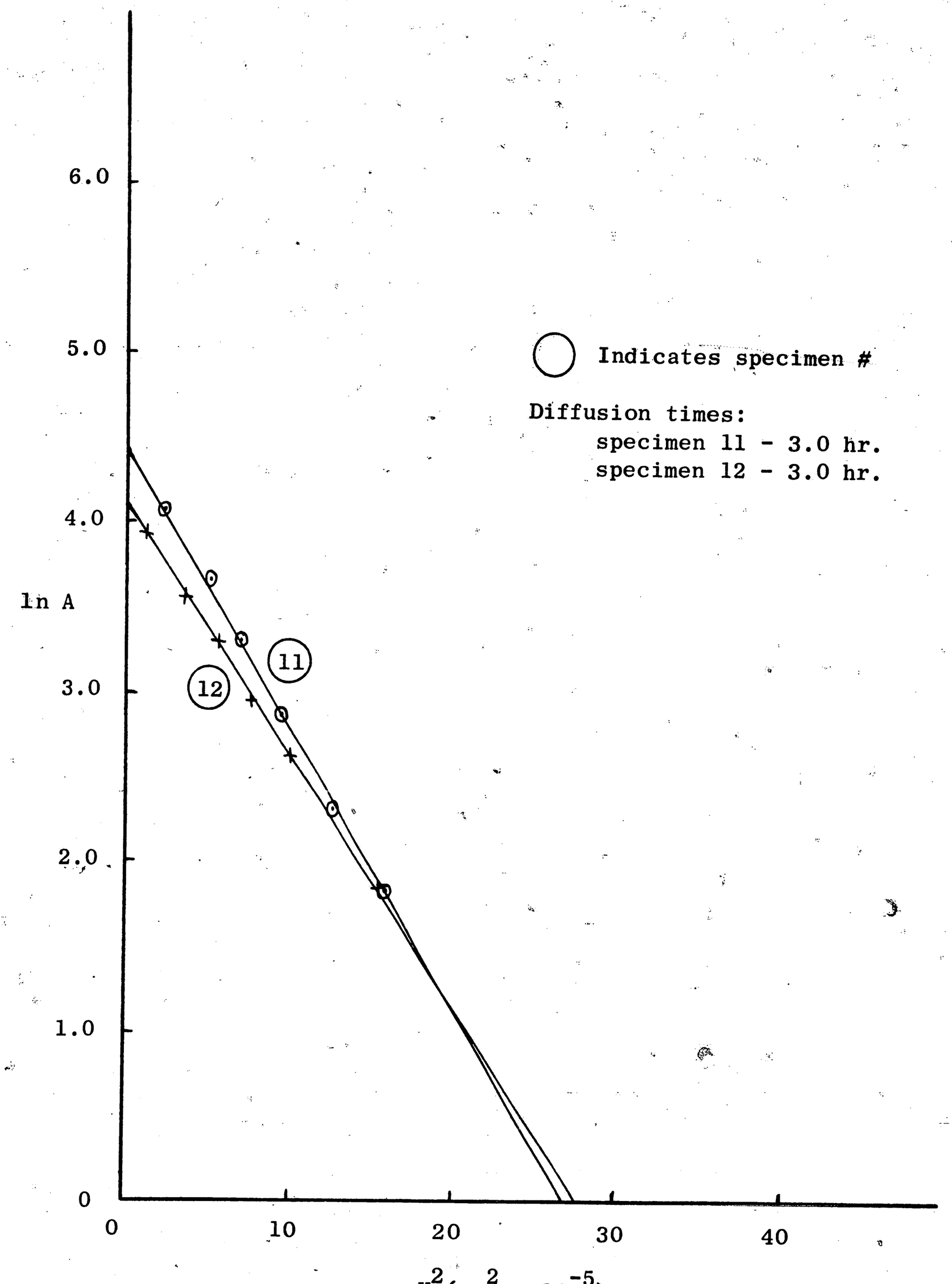

○ Indicates specimen #

Diffusion times:
specimen 11 - 3.0 hr.
specimen 12 - 3.0 hr.

FIGURE III-2

Plot of natural logarithm of Activity versus square of mean penetration distance for specimens diffused // basal plane at 620°K with ultrasonics // c axis.

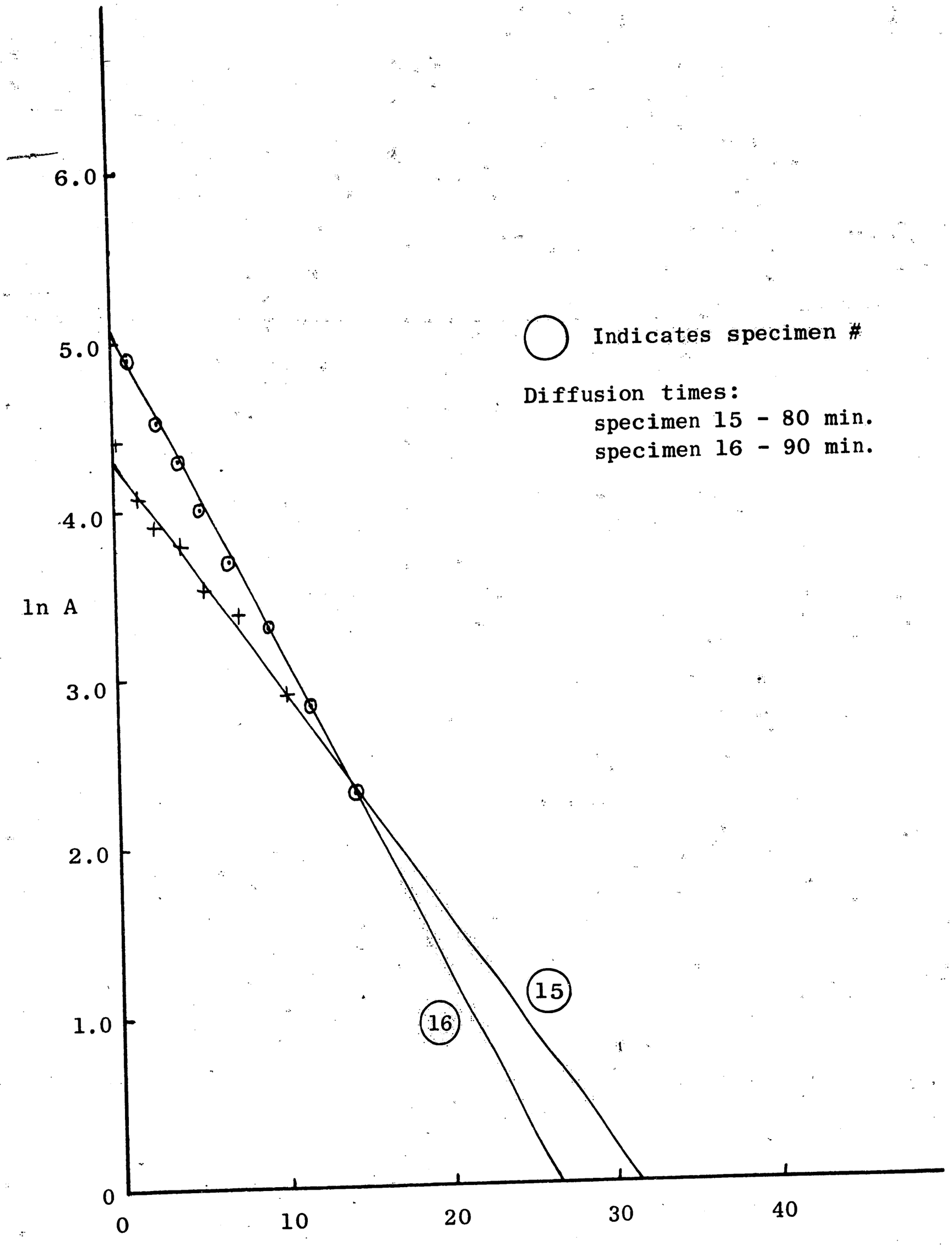

○ Indicates specimen #

Diffusion times:
specimen 15 - 80 min.
specimen 16 - 90 min.

FIGURE III-3

Plot of natural logarithm of Activity versus square of mean penetration distance for specimens diffused // c axis at 620°K without ultrasonics.

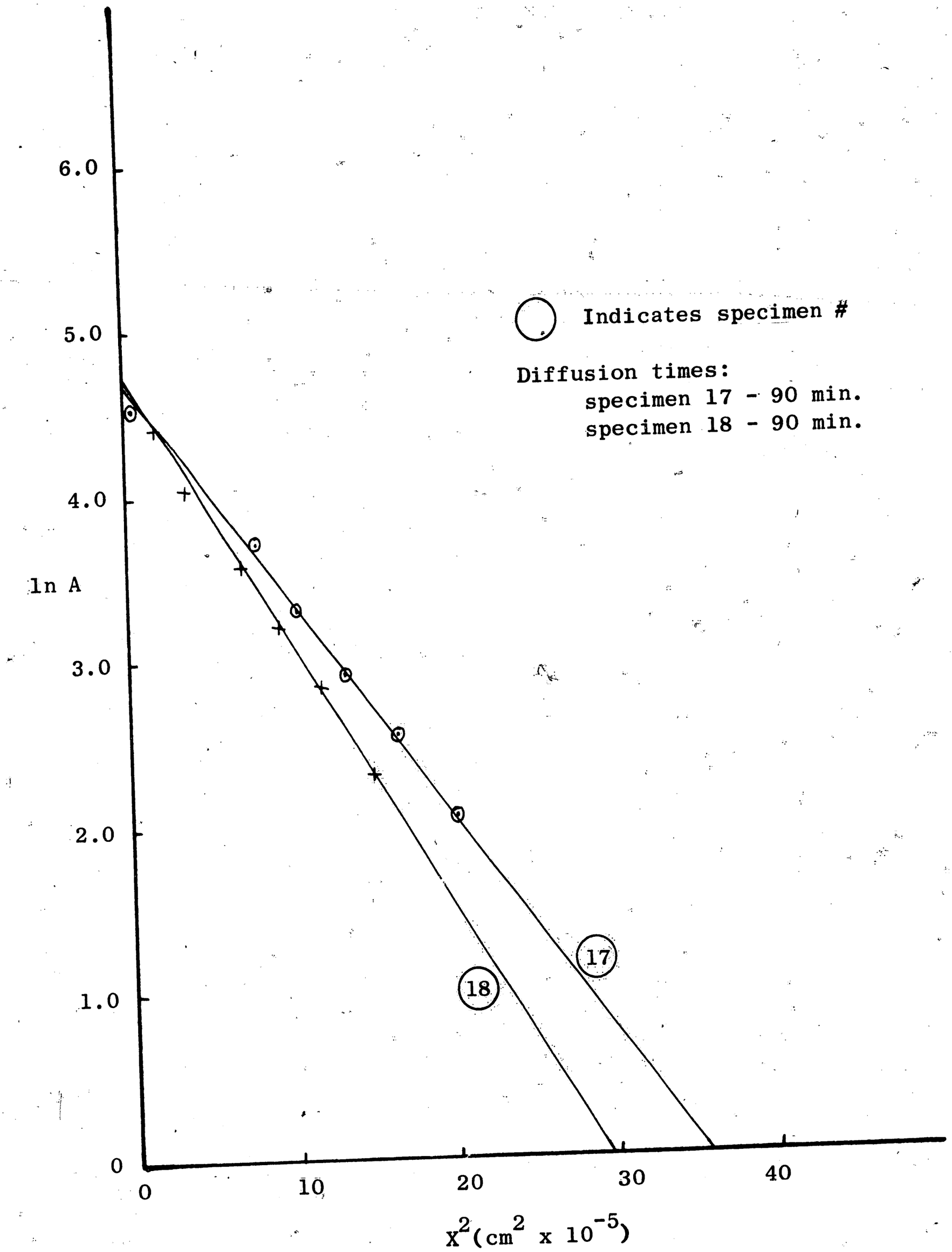

◯ Indicates specimen #

Diffusion times:
specimen 17 - 90 min.
specimen 18 - 90 min.

FIGURE III-4

Plot of natural logarithm of Activity versus square of mean penetration distance for specimens diffused // c axis at 620°K with ultrasonics // basal plane.

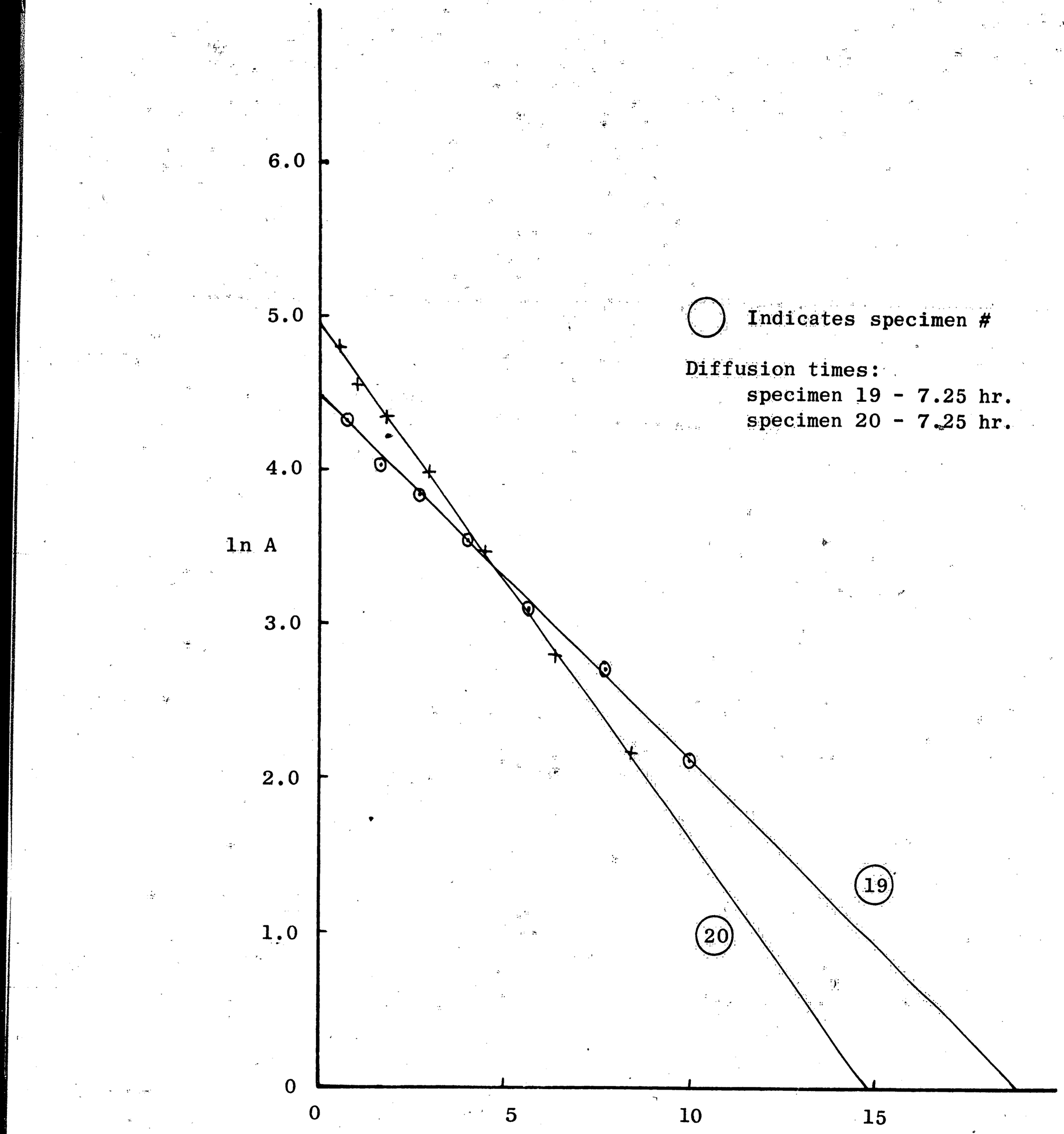

FIGURE III-5

Plot of natural logarithm of Activity versus square of mean penetration distance for specimens diffused // c axis at $550^{o}K$ without ultrasonics.

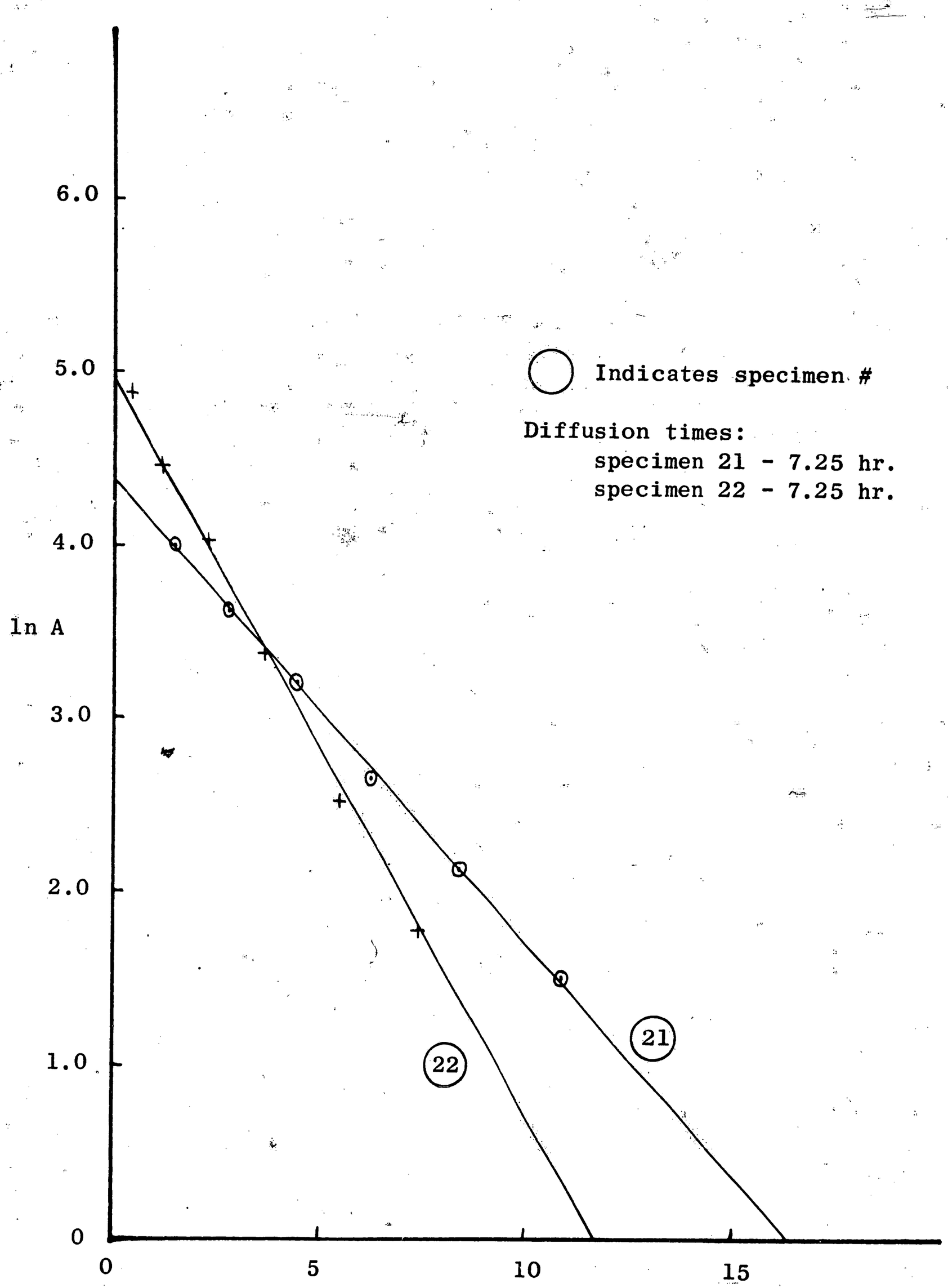

○ Indicates specimen #

Diffusion times:
specimen 21 - 7.25 hr.
specimen 22 - 7.25 hr.

FIGURE III-6

Plot of natural logarithm of Activity versus square of mean penetration distance for specimens diffused // c axis at 550°K with ultrasonics // basal plane.

APPENDIX IV

Sample Calculations For Sectioning and Counting

The data for sectioning and counting specimen 8 are given in Figure IV-1. The following calculations are taken from the final section on specimen 8:

1. Depth of Sectioning

The weight of material removed is equal to the difference between the specimen weight before and after lapping: 10647.4 - 10639.9 = 7.5 mg.

The depth of the section is calculated from the measured surface area, density of zinc, and weight of material removed:

$$\text{Volume} = \frac{\text{Wt.}}{\text{density}} = \frac{.0075 \text{ gm.}}{7.1 \text{ gm./cc}} = 0.001056 \text{ cc.}$$

$$\text{Depth} = \frac{V}{A} = \frac{10.56 \times 10^{-4} \text{ cc}}{0.795 \text{ cm}^2} = 13.3 \times 10^{-4} \text{ cm} = \underline{13.3 \text{ microns}}$$

2. Mean Penetration Distance

The mean penetration distance (X) is the distance from the initial surface of the specimen to the center of the section in question. This is obtained by summing up all the previously calculated section depths and adding one half of the depth of the section being measured:

$$X = 133.8 + \frac{13.3}{2} = \underline{140.45 \text{ microns}}$$

3. Activity

A total of 5000 counts was made on each section and the time

required for this number was recorded:

$$CPM = \frac{5000}{time} = \frac{5000}{38.9} = \underline{125.7 \text{ cpm}}$$

This figure must be corrected for normal background radiation, 39 cpm, in this case. Due to the variation in thickness of each section, the activity must be normalized by dividing by the section thickness, resulting in an activity in units of cpm/micron:

$$Activity = \frac{CPM-BKGRD}{Depth} = \frac{125.7-39}{13.3} = 6.52 \text{ cpm/micron}$$

Specimen 8 Area of Diffusion Surface = 0.795 cm^2

SECTIONING

Section	Specimen Wt. (mg.)	Section Wt. (mg.)	Section Depth (μ)	Cumulative Depth (μ)	X(μ)	$X^2(\mu^2)$
	10722.8					
1	10718.9	3.9	6.9	6.9	3.45	12
2	10709.7	9.2	16.3	23.2	15.10	228
3	10701.5	8.2	14.5	37.7	30.45	927
4	10693.0	8.5	15.1	52.8	45.25	2050
5	10685.6	7.4	13.1	65.9	59.35	3520
6	10678.3	7.3	13.0	78.9	72.40	5230
7	10670.6	7.7	13.7	92.6	85.75	7350
8	10663.1	7.5	13.3	105.9	99.25	9870
9	10655.4	7.7	13.7	119.6	112.75	12700
10	10647.4	8.0	14.2	133.8	126.70	16050
11	10639.9	7.5	13.3	147.1	140.45	19750

COUNTING (5000 counts)

Section	Time (min.)	CPM	Bkgrd. (cpm)	Act. (cpm/μ)	ln A
1	11.35	441	39	57.8	4.05
2	5.35	934	39	54.9	4.00
3	6.45	776	39	50.8	3.93
4	7.88	635	39	39.4	3.675
5	9.13	548	39	38.8	3.66
6	10.48	477	39	33.7	3.515
7	13.54	369	39	24.1	3.18
8	17.23	290	39	18.9	2.935
9	21.17	236	39	14.4	2.665
10	29.04	172	39	9.37	2.235
11	38.90	125.7	39	6.52	1.875

Figure IV-1

Data Sheet for Sectioning and Counting of Specimen 8

BIBLIOGRAPHY

1. Schenck, H. and E. Schmidtmann, Archiv fur das Eisenhuttenwesen, Vol. 25, No. 11/12, pp. 579-583, 1954, Henry Brutcher Translation (HB 3500).

2. Rozanski, W., Archivum Hutnictwa, Vol. 3, No. 2, pp. 125-146, 1958, Henry Brutcher Translation (HB 4860).

3. Tanaka, S., T. Yoshida and K. Tagaki, Tetsu To Hagane, Vol. 35, 931, 1952, Henry Brutcher Translation (HB 4157 and 4158).

4. Pogodin-Alekseev, G., Metallovedenie i Obrabotka Metallov, No. 6, pp. 14-17, June 1958, Henry Brutcher Translation (HB 4247).

5. Ermakov, V. and E. Al'ftan, Metallovedenie i Obrabotka Metallov, No. 7, pp. 22-27, July 1958, Henry Brutcher Translation (HB 4278).

6. Schoenthaler, D., An Analysis of the Effects of Ultrasonics on Diffusion and the Diffusion of Copper Acceptors in Germanium, Master's Thesis, Lehigh University, June 1965.

7. Al'ftan, E., Nauchn. Doklady Vyssh. Shkoly-Metallurgiya, No. 1, pp. 19-24, Jan./Mar. 1959, Henry Brutcher Translation (HB 4715).

8. Balalaev, Yu. F., Metallovedenie i Term. Obrabotka Metallov, No. 1, pp. 48-49, Jan. 1964, Henry Brutcher Translation (HB 6181).

9. Miller, P. H. and F. R. Banks, Phys. Rev., Vol. 61, 648, 1942.

10. Liu, T. and H. G. Drickamer, J. of Chem. Phys., Vol. 22, No. 2, 312, 1954.

11. Mason, W. P., Physical Acoustics and Properties of Solids, D. Van Nostrand, Princeton, 1958.

12. Shewmon, P. G., Diffusion in Solids, McGraw-Hill, New York, 1963.

13. Crank, J., The Mathematics of Diffusion, Oxford University Press, London, 1956.

14. Cullity, B. D., Elements of X-ray Diffraction, Addison-Wesley, Reading, Mass., 1959.

VITA

Brian F. Walker was born May 27, 1934 in Detroit, Michigan to Mr. and Mrs. L. L. Walker. Upon graduation from Detroit Catholic Central High School in 1952, he received an appointment to the United States Naval Academy. He graduated from the Naval Academy and was commissioned Ensign in the U. S. Navy in June 1956.

After serving four years on active duty in the Navy, Mr. Walker was released from active duty and joined the Western Electric Company, Installation Division, in Detroit, Michigan. In 1962, he transferred to the Engineer of Installation in New York City, working in the Methods group. In 1964, he was selected by Western Electric to attend Lehigh University and study for a Master of Science degree in Metallurgy and Materials Science.